

# Tumor-Targeting Oxidative Stress Nanoamplifiers as Anticancer Nanomedicine with Immunostimulating activities

*Nanhee Song*<sup>1,#</sup>, *Miran Park*<sup>1,#</sup>, *Yeungjong Lee*<sup>1</sup>, *Yujin Lee*<sup>1</sup>, *Eunkyeong Jung*<sup>2</sup>,

*Dongwon Lee*<sup>1,3,\*</sup>

<sup>1</sup> Department of Bionanotechnology and Bioconvergence Engineering, Jeonbuk National University, Baekjedaero 567, Jeonju, Jeonbuk, 54896, Republic of Korea

<sup>2</sup> Department of NanoEngineering, University of California San Diego, La Jolla, 92093, CA, USA

<sup>3</sup> Department of Polymer Nano Science and Technology, Jeonbuk National University, Baekjedaero 567, Jeonju, Jeonbuk, 54896, Republic of Korea

# These authors equally contributed in this work.

**Corresponding Authors:** Dongwon Lee, [dlee@chonbuk.ac.kr](mailto:dlee@chonbuk.ac.kr)

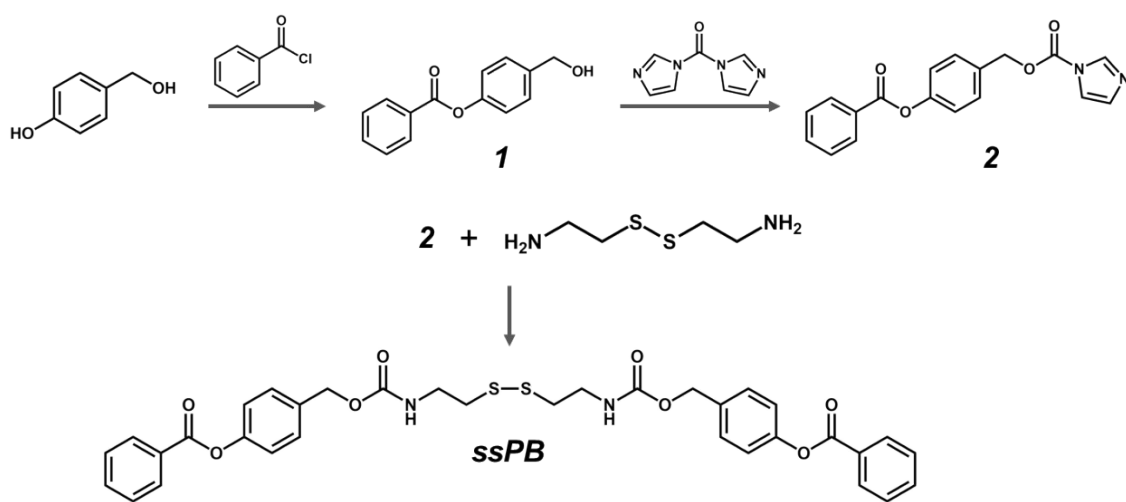


Figure S1. A synthetic route of ssPB.

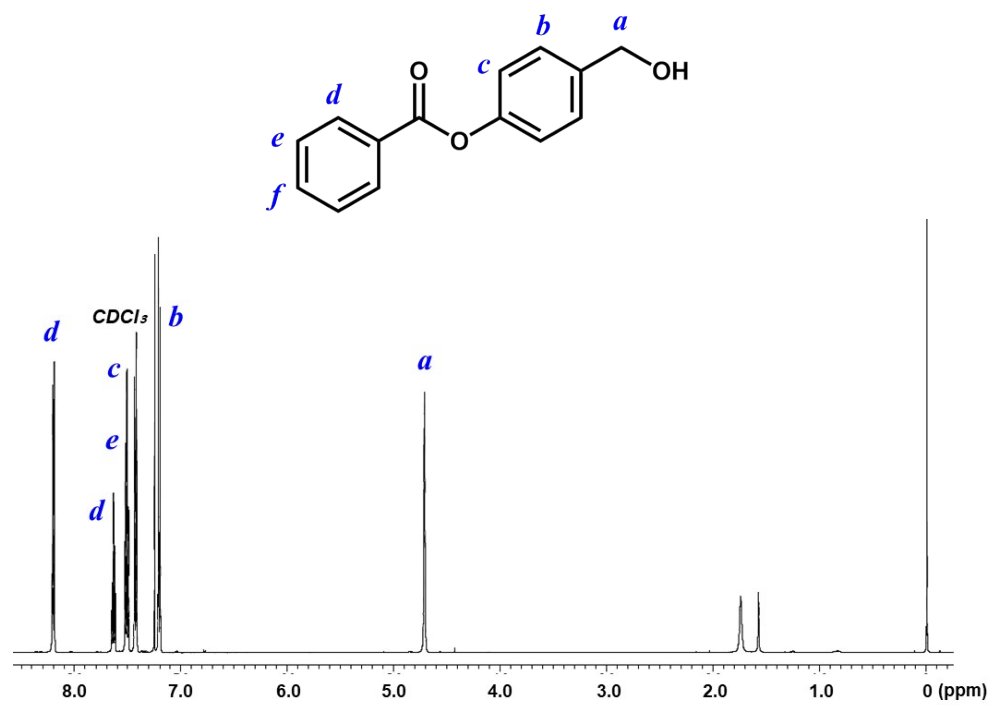


Figure S2. <sup>1</sup>H NMR spectrum of Compound **I** recorded in CDCl<sub>3</sub>.

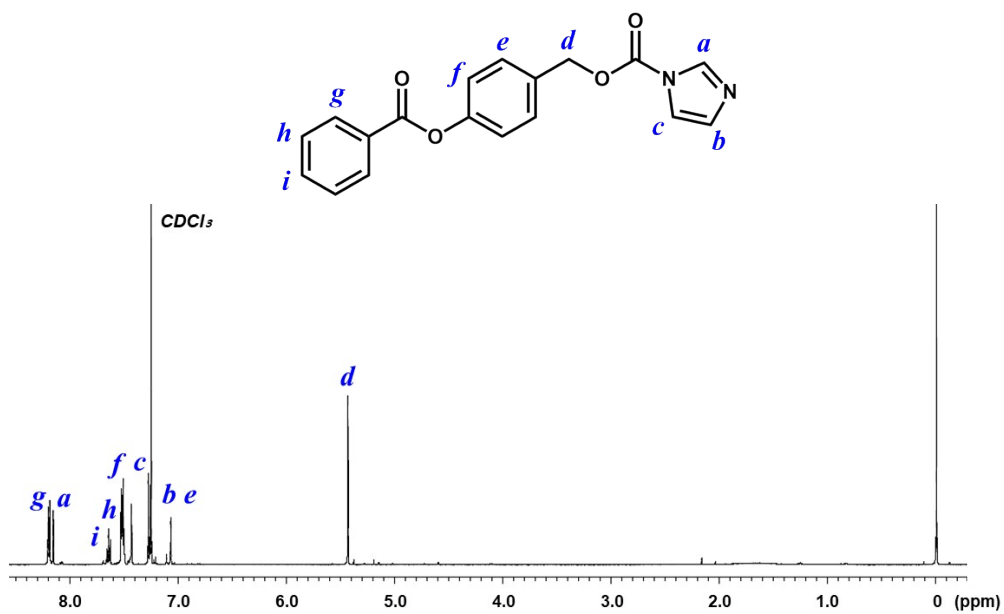


Figure S3. <sup>1</sup>H NMR spectrum of Compound 2 recorded in CDCl<sub>3</sub>.

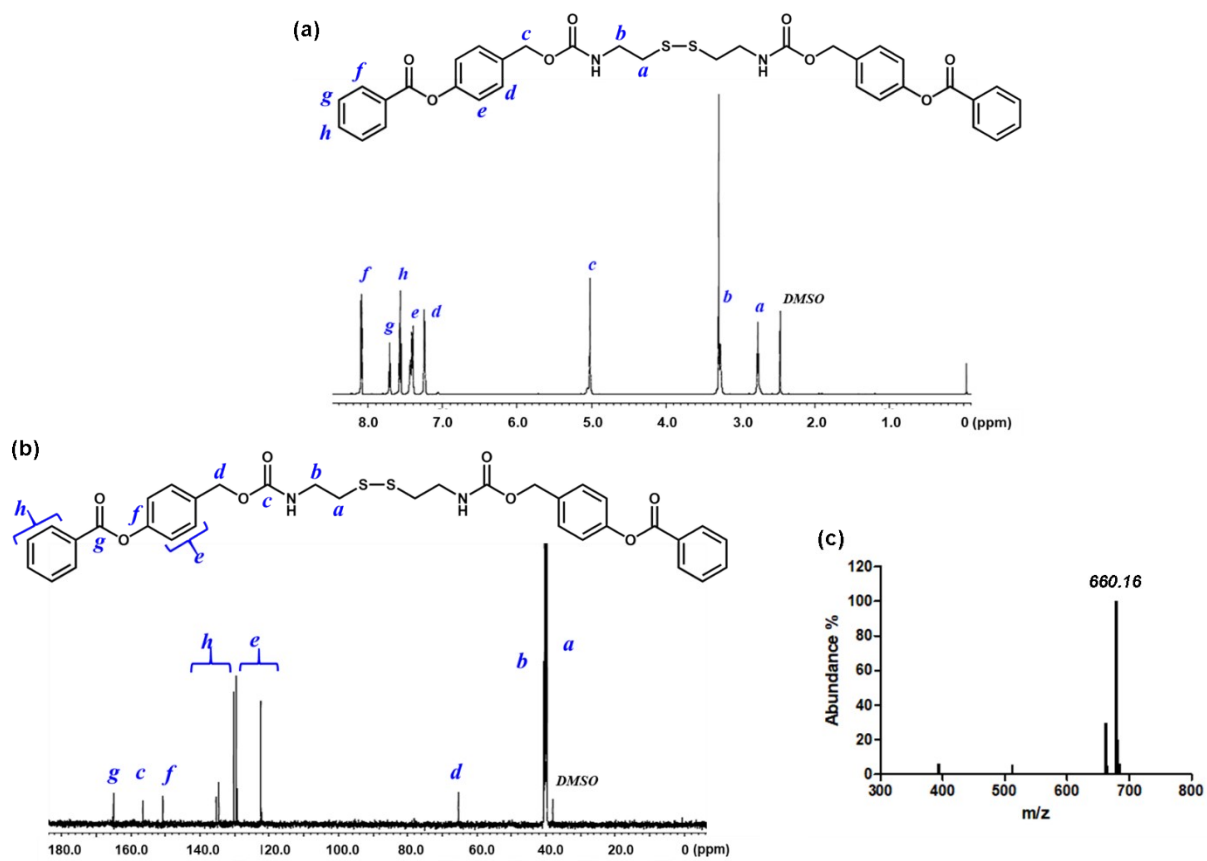


Figure S4. Characterization of ssPB. (a)  $^1\text{H}$  NMR spectrum and (b)  $^{13}\text{C}$  NMR spectrum. (c) LC/MS spectrum.

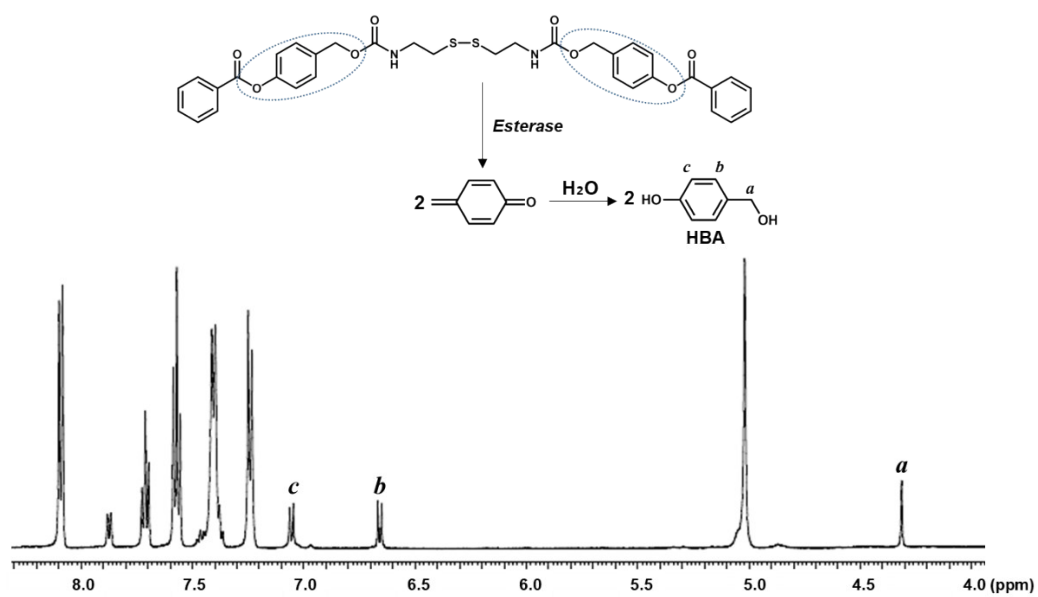


Figure S5. <sup>1</sup>H NMR spectrum of ssPB after esterase-triggered hydrolysis under aqueous condition.

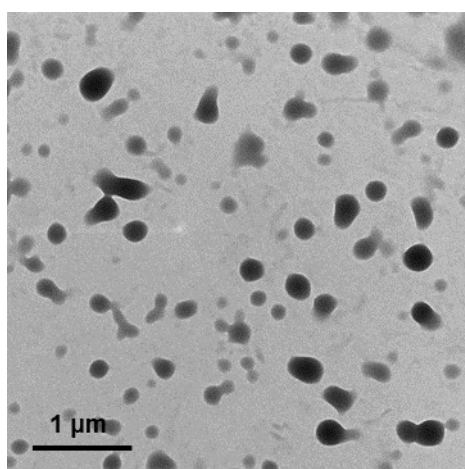


Figure S6. TEM micrograph of F-ssPB nanoassemblies dispersed in PBS.

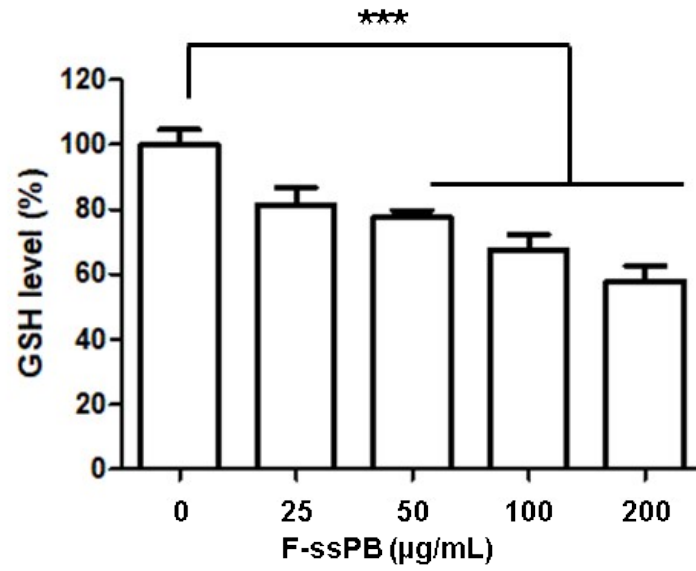


Figure S7. Depletion of GSH by F-ssPB nanoparticles in DU145 cells. Values are mean  $\pm$  s.d.

(n=4). \*\*\* p<0.001.



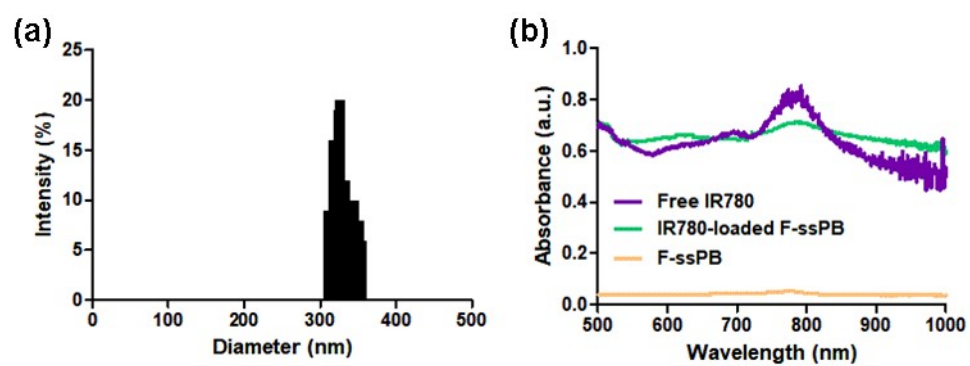


Figure S8. Characterization of IR780-loaded F-ssPB nanoparticles. (a) Size and size distribution determined by dynamic light scattering. (b) UV-vis absorbance.

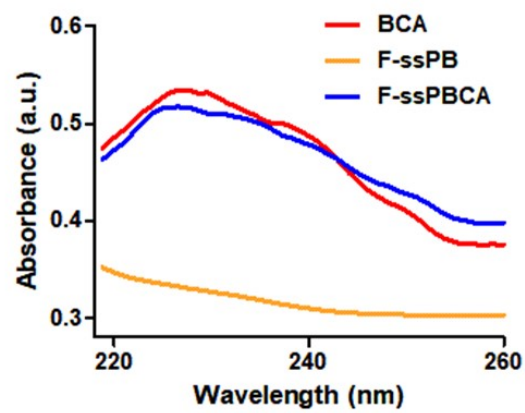


Figure S9. UV absorbance of BCA, F-ssPB and F-ssPBCA.

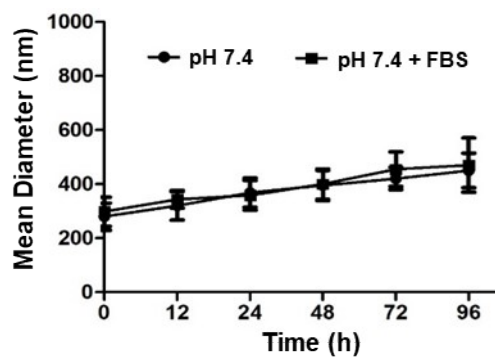


Figure S10. Changes in the hydrodynamic diameter of F-ssPBCA nanoparticles during incubation in the presence or absence of FBS (10 wt%).

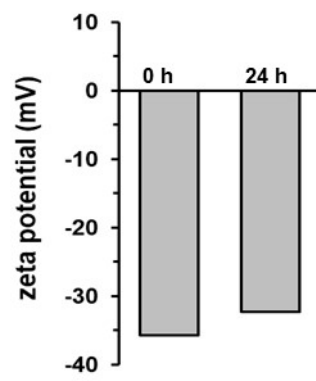


Figure S11. Zeta potential of F-ssPBCA nanoparticles dispersed in PBS.

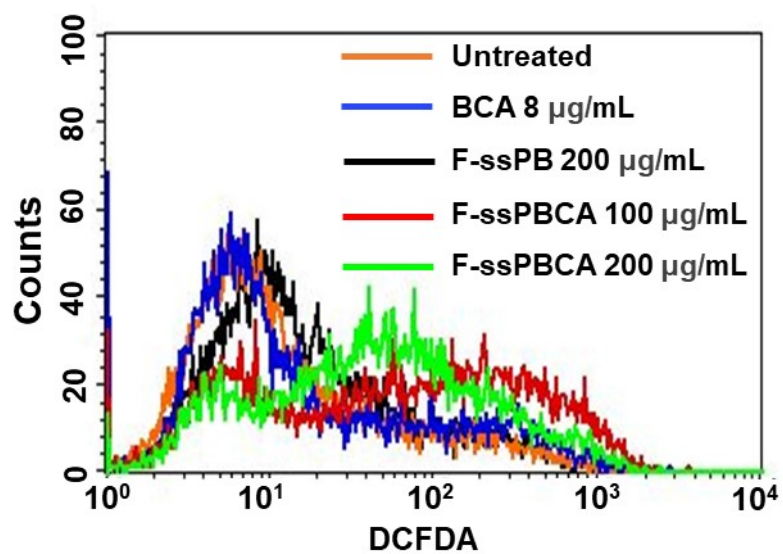


Figure S12. Flow cytometric analysis of ROS accumulation in cells treated with BCA, F-ssPB and F-ssPBCA nanoparticles.

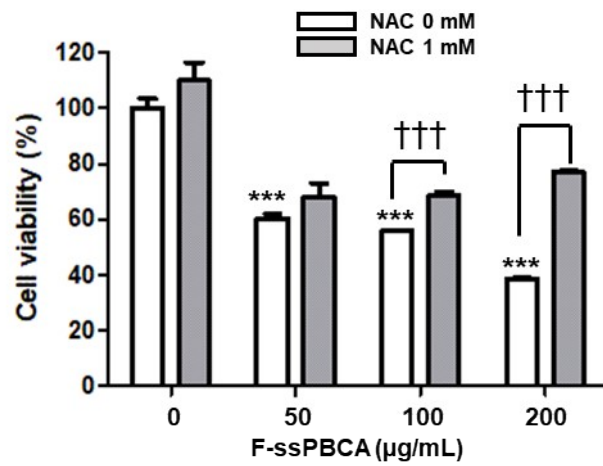


Figure S13. The effects of antioxidant NAC on the cytotoxicity of F-ssPBCA nanoparticles against DU145 cells. Values are mean  $\pm$  s.d. (n=4). \*\*\* p<0.001 relative to F-ssPBCA 0 µg/mL.

††† p<0.001.

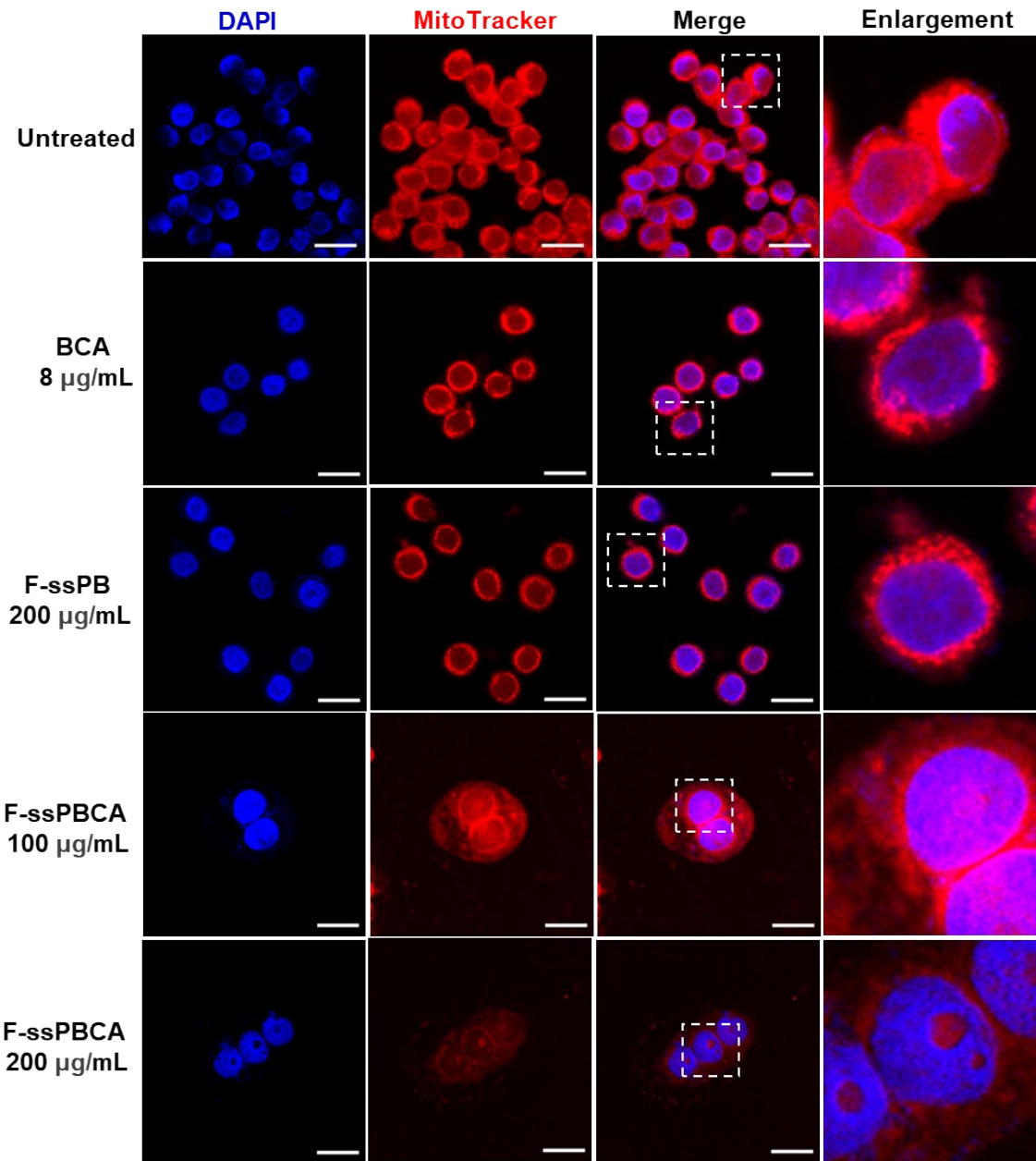


Figure S14. Fluorescence images of cells stained with MitoTracker Red. Nuclei were stained with DAPI. The scale bar is 20  $\mu\text{m}$ .

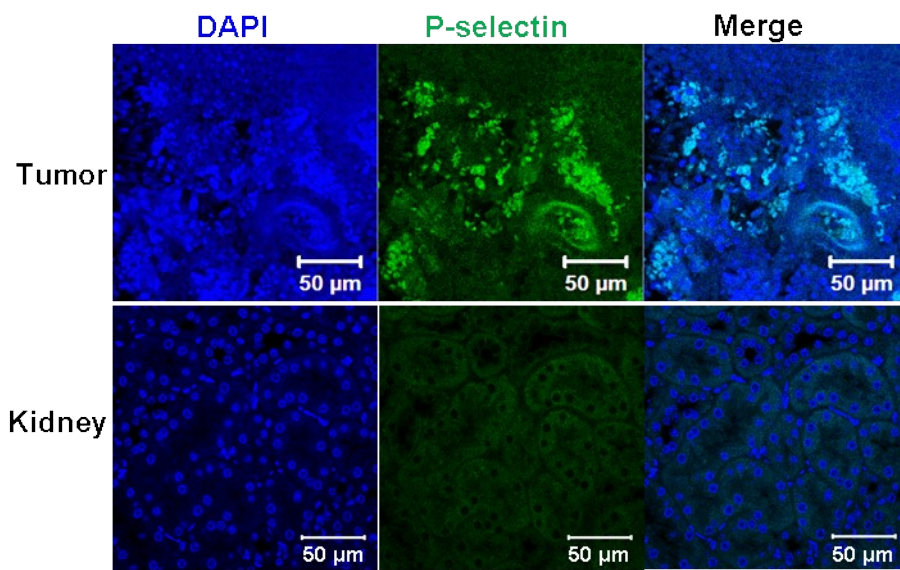


Figure S15. Immunofluorescence images of SW620 tumor and kidney tissues stained with p-selectin antibody and DAPI.



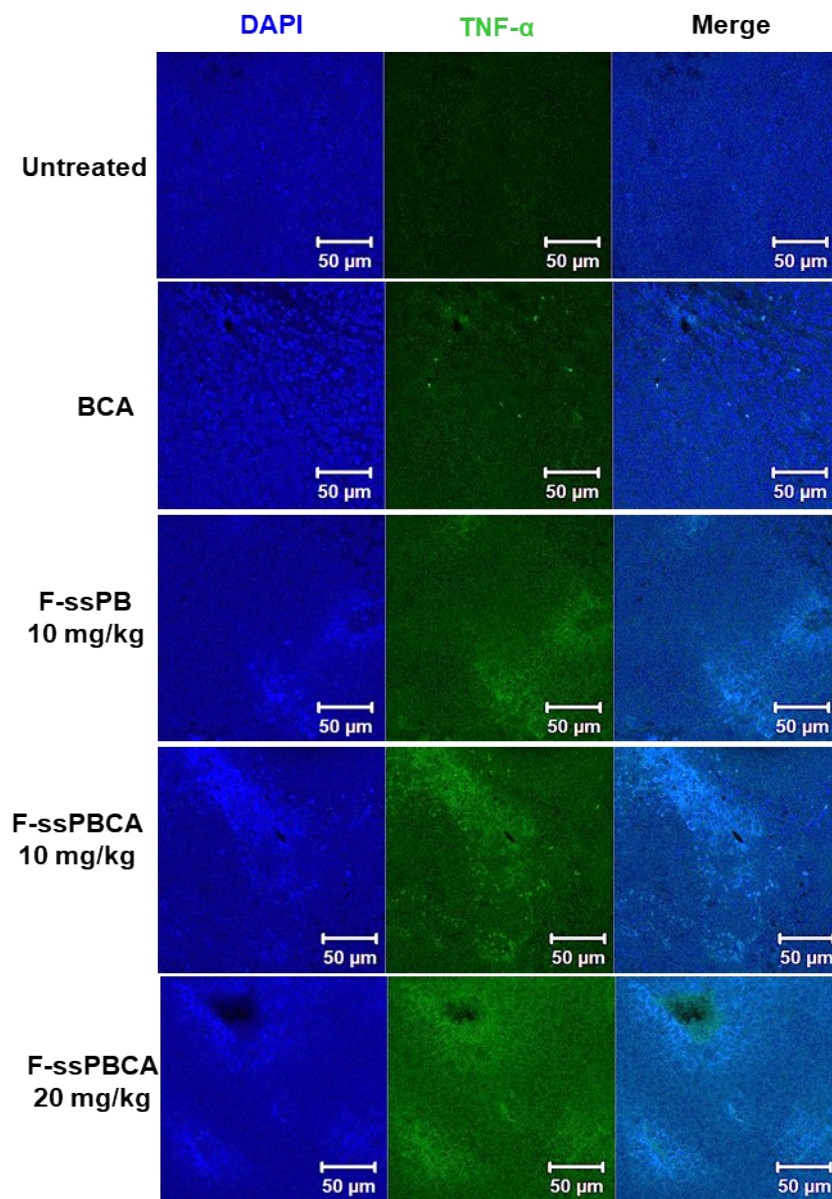


Figure S16. Micrographs of tumor tissues stained with anti TNF- $\alpha$ .

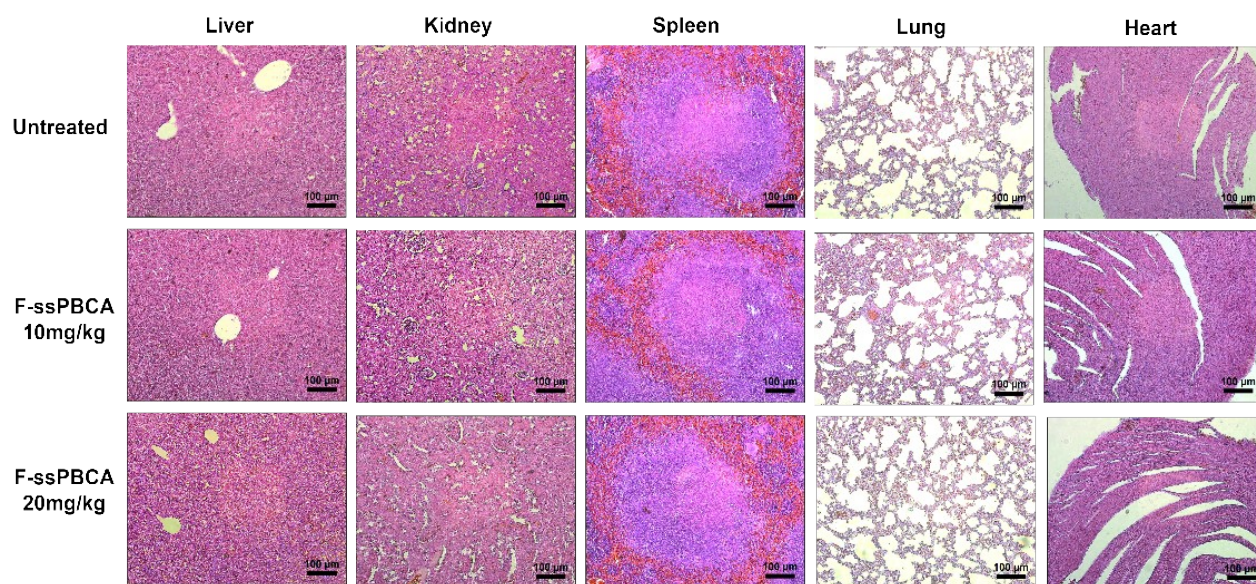


Figure S17. Representative H&E staining images of major organs from various groups. Tissues were excised after finishing *in vivo* study.

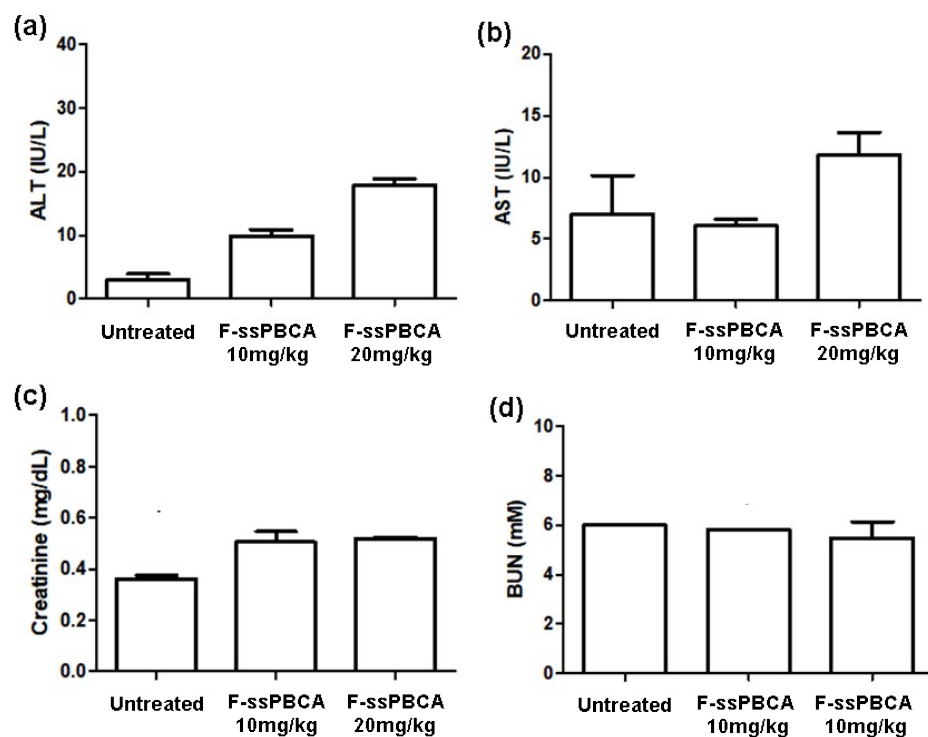


Figure S18. The effects of F-ssPBCA nanoparticles on hepatic and renal functions. (a) ALT, (b) AST, (c) creatinine and (d) BUN. Data are represented as the mean  $\pm$  SD.